

Measuring Anisotropic Light Scatter within Graphic Arts Papers For Modeling Optical Dot Gain

Kathrin Happel, Marius Walter, Philipp Urban, Edgar Dörsam
 Institute of Printing Science and Technology, Technische Universität Darmstadt, Germany
 happel@idd.tu-darmstadt.de

Abstract

Optical dot gain (ODG) plays an important role for predicting the color of printed halftones. The detailed knowledge of light scatter within the printing substrate might improve the accuracy of printer models and can reduce the number of required training colors to fit the model to the printing system.

We propose an apparatus and method for measuring local anisotropic light scatter within graphic arts paper for predicting ODG. The setup is a modification of existing approaches for a more robust determination of the light's point spread function (PSF). To verify our approach we develop a simplified color prediction model for printed halftones that is based only on the reflectances of the fulltone color and the paper and incorporates the PSF for modeling the ODG. Our experiments show that the accuracy of the model in terms of color differences to the measured colors was improved by considering ODG.

Introduction

The reflectance spectrum of a print reproduction is a result of various factors including the spectral reflectance properties of inks and papers, the scattering behavior of incident light within the paper as well as the considered printing process and halftone method. Printing system properties such as the printer gamut or the optical dot gain (ODG) directly depend on these factors.

In order to correctly control a printing process we need a mathematical model of the printer that accurately predicts spectral reflectances of the printout given a particular set of control values.

We can find a wide variety of models for predicting spectral reflectances of multi-ink prints in literature. Wyble and Berns [1] distinguish two general types of printer models: *regression based models* and *first principle models*. They state that most models used in practices are *regression based models*. These models simulate the behavior of the system as a whole and are not necessarily based on physical principles. In general, test patches are printed and the model parameters are fitted to the reflectances measured.

If one of the influencing factors, such as ink, paper or the printing process is changed, new test patches have to be printed and the model parameters have to be fitted again. It is very difficult to calculate correction factors to transfer the printer model to a different setup. Furthermore, the number of test patches required for accurately fitting the model to a setup usually increases drastically with the number of inks. The frequently used *cellular Yule-Nielsen spectral Neugebauer model* (CYNSN) [6, 7, 8, 9] with x grid points requires x^k test patches, where k is the number of inks. Modeling a four-ink system utilizing five grid points results in 625 test patches. For a seven-ink system the number of test patches increases to 78,125. The measurement effort as well

Expenses for fitting a printer model

number of inks	number of test patches	area covered with test patches (5mm x 5mm)
4 (CMYK)	625	0.0156 m ²
7 (CMYKRGB)	78,125	1.95 m ²

as the required resources in terms of consumables to print these test patches exceed any practical dimension (see table).

In recent years printing with seven (CMYKRGB) and more inks became increasingly important and new printers such as the Canon imagePROGRAF IPF6100 or HP Z3200 with up to 12 inks were introduced to the market. The described drawbacks of regression based models limit their applicability for those systems.

In contrast, *first principle models* simulate the physical processes of the printing system. Even if we consider a printing system with more than four inks we can assume that only a few test patches are required to fit a first principle model. In this case, the overall number of model parameters of the first principle model should be significantly smaller than the number of parameters of the regression based model ($j + k \ll m$ see figure 1). Additionally, some of the results might be transferable to other printing setups. If only the paper differs, all parameters that are paper-independent have not to be changed. Hence, it is plausible that the effort for fitting a model to a setup can be reduced drastically using a first principle model.

To better understand the concept of first principle models we need to look closer at the printing process: A raster image processor (RIP) calculates a digital halftone pattern from the printer control values (figure 1). The printer creates a physical image of this pattern onto the paper (concept images in figure 1). Usually,

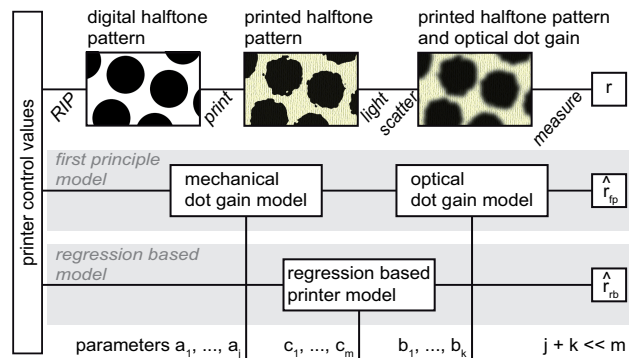


Figure 1. Printing process and two different types of printer models

the dots on paper are larger than intended. This phenomenon is called ink spread and is influenced by the printing machine and by ink paper interactions. But this spatial ink distribution does not directly correlate with the reflectance spectra that can be measured. The measured dots seem to be larger than expected. This is called the ODG and is caused by light scatter in paper. This optical phenomenon influences human observation and measurements. In figure 1 a first principle model is presented that models ink spread and ODG separately, combining a mechanical dot gain model with an ODG model. In this paper we focus on the optical and do not investigate the mechanical dot gain.

It is consensus within the scientific community that modeling ODG is a key element of an accurate printer model. There have been various approaches for describing light scattering [2, 3] and models for the combined effects of absorption and scattering [4, 5]. But the measurement of real light scattering in paper is difficult. Most models, regression based and first principle respectively, combine physical and empirical approaches. An example is the Yule-Nielsen model. Considering the ODG, Yule and Nielsen have introduced an empirical factor [10] that was incorporated into the Neugebauer model. Experiments show that considering ODG using this Yule-Nielsen "n"-factor improves the accuracy of the Neugebauer model significantly [11].

For this reason, detailed investigations were conducted to relate the ODG to physical properties of the printing process [12, 13, 14]. An important factor is the light's *point spread function* (PSF) that describes the photon migration within the paper. Knowing the PSF allows us to model the ODG by convoluting the halftone pattern (after ink spread) with the PSF (see figure 2). Hence, the PSF is the key parameter that enables us to separate the mechanical from the ODG as shown in figure 1.

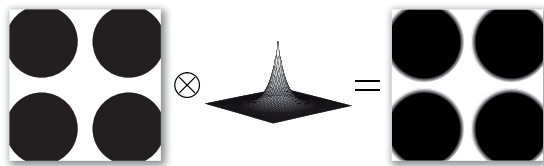


Figure 2. ODG as a convolution of a test pattern with a PSF

A PSF measurement setup has been proposed by Yule and Nielsen [10], where a tungsten filament was projected onto the paper's surface. The light descent of the ideally sharp edge of the filament is related to the light scattering in the paper and was observed through a microscope. Later, they suggested to project a sharp edge of a blade, thusly generating a sharply edged shadow zone. The blade was inserted into the light beam of a microdensitometer. Arney et al. [15] used a CCD chip for detection and changed the illumination angle from 45° to 20°. The disadvantage of the 45° angle was the effect of shadowing of the paper fibers caused by the rough surface. This could be resolved, when Ackermann et al. [16] chose a 0°/0° measurement setup by using the beam splitter of a microscope. He also used a CCD camera for detecting the projected edge of a razor blade. In this work, a method for measuring the light scattering in paper is presented, which is based on the measuring methods described above. [17] In contrast to previous approaches, our method shows the following improvements:

1. It is not necessary to know the position of the edge of the dark zone exactly in order to derive the point spread properties of the sample paper.
2. A sample holder allows for simple and accurate focusing.
3. Angular anisotropic scattering can be measured by rotating the sample holder around the vertical axis of the microscope.

To validate our method we present example measurements that show good correlation to the ODG of printed AM halftones.

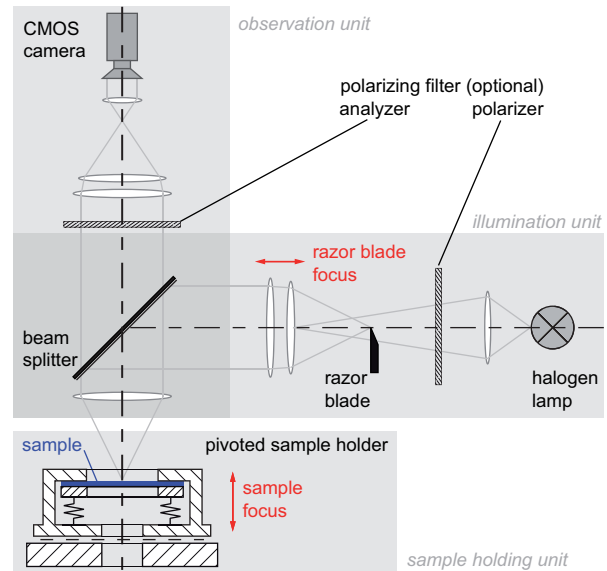


Figure 3. Measurement setup

Measurement Setup

To measure the *PSF*, a microscope was modified according to figure 3. The setup consists of three logical parts: an illuminating unit, an observation unit, and a sample holding unit (figure 4). As illumination, a halogen lamp provides a continuous spectrum. A razor blade, inserted into the light path generates an illuminated and a shadowed region. The razor blade focus allows the resulting image being sharply projected onto the sample surface. The beam splitter deflects the shadow image, projecting it onto the sample in 0° illumination angle. For observation, the image passes the beam splitter and can be recorded with a camera in a 0° observation angle. We used a CMOS RGB camera, evaluating only the green pixels. The pixel rows of the camera are aligned to the projected edge. Two slots allow for optional polarization filters that can be inserted into illuminating unit and observation unit respectively. The direction of polarization of the filter of the illuminating unit can be adjusted to be parallel or orthogonal to the filter of the observation unit.

The sample holder (figure 4) is divided into two parts. The first part holds the reference, i.e. a mirror or a defined rough reflector, the second part holds the sample. Both, sample and reference are beared against the front plate of the holder, fixed with springs. Thusly, the surfaces of sample and reference are nearly perfectly aligned. After focusing the reference surface and taking the reference image, no focus corrections need to be made for the sample. The sample holder is moved sideways until the sample is in the observation path. Now, all measurement images can be

acquired. For anisotropic measurements, the sample holder can be rotated around the vertical axis of the microscope, e.g. in 10° steps.

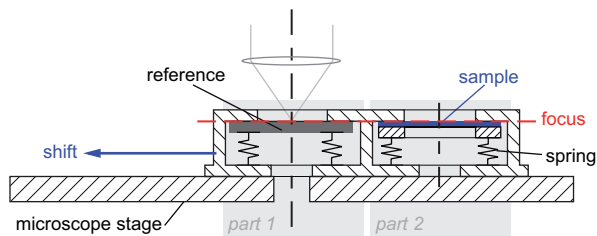


Figure 4. Sample holder; reference part (1) and sample part (2)

Measuring Anisotropies of Sample Papers

For each of the 36 angles, investigated for each paper, a 2D image is captured. In a preliminary step the rows of the image can be averaged along the direction of the edge without losing any important information. This reduces noise and redundant data significantly. The output of this computation is referred to as the sample edge spread function (ESF) E in the following (see figure 10).

For our measurements we used three wood-free graphic arts papers typically employed for offset printing:

1. LumiArt (StoraEnso), 115g/m², glossy coated
2. LumiSilk (StoraEnso), 115g/m², matt coated
3. MaxiOffset (Igepa), 80g/m², uncoated

Qualifying the anisotropies of the measurements, we used the distance $x_{0,1}$. This value is defined as the distance from the mean of the ESF to the point, where the ESF has dropped to 10% of its maximum. For visualization purposes a polar diagram features the clearest presentation of anisotropies, performing as an indicatrix of isolines. Figure 5 shows the 10%-indicatrices of all three papers and their mean radius in dotted lines. The radius is scaled in pixel of the camera. As it can be seen, paper 1 and paper 2 feature almost isotropic scattering. A slightly bigger deviation from an isotropic circle can be found for paper 3, the uncoated paper.

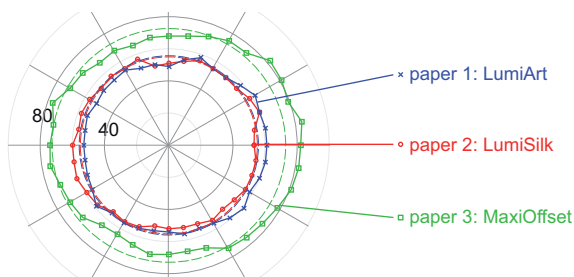


Figure 5. 10% isolines as indicatrices for anisotropies of the sample papers

In the following calculations, these anisotropies will be neglected. The assumption of isotropic scattering is reasonable, especially if we consider a certain noise in the measurements. Thus, for each paper, the computations are based on the mean of the measured ESFs over all angles.

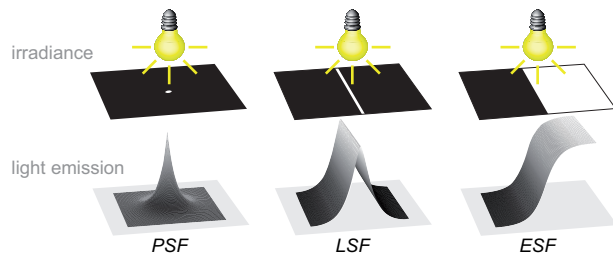


Figure 6. PSF, LSF, and ESF; irradiance and corresponding emission of a sample with scattering properties

Deriving the LSF and PSF

Three spread functions (figure 6) have to be considered for describing scatter within paper: point spread function (PSF) $P(r)$, line spread function (LSF) $L(x)$, and edge spread function (ESF) $E(x)$. If scattering is isotropic, the relation between the three spread functions can be described [18] according to equations 1-4.

$$L(x) = \frac{d}{dx} E(x) \quad (1)$$

$$E(x) = \int_{-\infty}^x L(\xi) d\xi \quad (2)$$

$$P(r) = -\frac{1}{\pi} \int_r^{\infty} \frac{L'(x)}{\sqrt{x^2 - r^2}} dx. \quad (3)$$

$$L(x) = 2 \cdot \int_x^{\infty} \frac{r \cdot P(r)}{\sqrt{r^2 - x^2}} dr \quad (4)$$

Some requirements have to be satisfied for measuring the ESF with the measurement setup introduced above: the illumination and the CMOS quantum efficiency of the camera have to be spatially homogeneous or at least known for correction. Additionally, Fresnel diffraction at the razor blade and other optical scatter or absorption properties of the microscope need to be considered. It is extremely difficult (if not impossible) to project an ideally sharp shadow edge onto the paper and accordingly, to know the position of the edge exactly.

Therefore, the direct measurement of the ESF and deriving the PSF analytically according to equations 1-3 is hard to handle. Instead, the PSF can also be approximated. In a first step, the razor blade has to be projected onto the reference surface (mirror or a defined rough reflector). The corresponding camera image is assumed to be the best achievable edge image and its mean along edge direction is called *reference ESF* (E_{ref}) in the following. We assume that light scatter within the reference material is negligible and has no influence on the reference ESF. All differences from an ideally step-like image are caused by internal reflections in the microscope, inhomogeneous illumination and possible diffraction at the razor blade edge. The second step is to take images of the edge projections onto our sample. We assume that all optical perturbations stay the same. In this case, the *sample ESF* (E) must be a convolution of the reference ESF E_{ref} with some unknown function F .

If diffuse surface reflections and other unknown errors are small and can be neglected, the function F is the LSF. Thus, it could be derived from the reference and sample ESF by deconvolution. Unfortunately, the noise of the images makes deconvolution

lution difficult and a solution is afflicted with uncertainty. Therefore, some more information about PSF and LSF is required. In literature we find different ansatzes (approaches) for light scatter within paper [2, 3], summarized by Berg [4]. We will concentrate on the ansatzes for isotropic PSFs and corresponding LSFs utilizing one parameter σ shown in the following table:

Different PSFs and corresponding LSFs

j	$P_j(r)$	$L_j(x)$
1	$\rho_1 \cdot \exp(-u^2/2)$	$\approx \rho_1 \sigma \sqrt{2\pi} \cdot \exp(-v^2/2)$
2	$\rho_2 \exp(-u)$	$2\rho_2 x \cdot K_1(v)$
3	$\rho_3 / (1+u^2)$	$\rho_3 \pi \sigma / \sqrt{1+v^2}$
4	$\rho_4 / (1+u)^2$	$2\rho_4 \sigma \frac{v^2 (\frac{\pi}{2} - \sin^{-1} v^{-1}) - \sqrt{v^2-1}}{(v^2-1)^{3/2}}$

where $u = r/\sigma$ and $v = x/\sigma$. Using these ansatzes we can write the convolution of the reference ESF as:

$$E_j = E_{ref} \otimes L_j \quad (5)$$

We also added ansatz 4, which decreases proportionally to the square of the radial distance. This type of equation is commonly used in physics, e.g. for the decrease of electromagnetic fields or sound. Any parameter σ defines a PSF and an LSF that can be convoluted with the reference ESF E_{ref} according to equation 5, and compared to the sample ESF E , using the root-mean-square deviation (RMSD). In this case, the RMSD is a measure of the approximation accuracy. We used this RMSD as the objective function for our optimization, varying the parameter σ . The parameter ρ_j is a scaling factor that differs from ansatz to ansatz. It depends only on σ and is chosen to satisfy the energy conservation:

$$\int_{-\infty}^{\infty} L(x) dx = 1 \quad (6)$$

Figure 7 shows an independent representation of the PSFs of ansatzes 1 to 4: the ordinate is the independent PSF $P \cdot \sigma$, the abscissa is the independent radius r/σ .

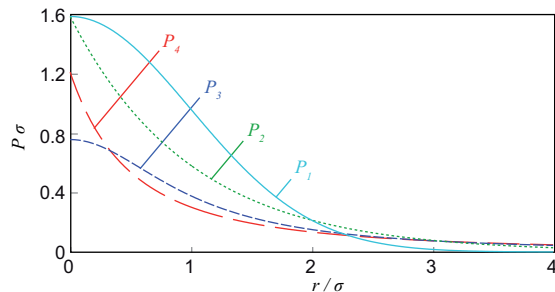


Figure 7. Representation of the PSFs according to the different ansatzes

The main advantage of this method compared to the analytical approach of equations 1-4 is that the knowledge of the exact position of the edge is not required for determining the PSF.

Figure 8 shows the algorithm for computing the LSF according to a chosen ansatz with the optimized parameter σ_{end} .

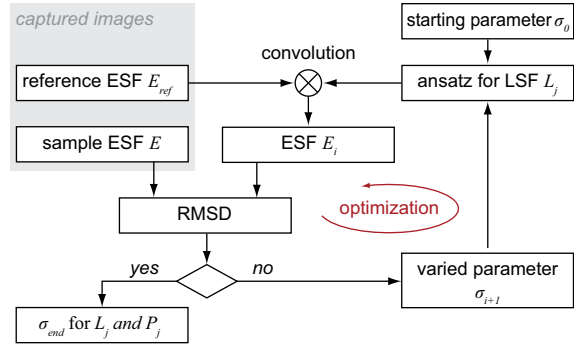


Figure 8. Computation algorithm for deriving an optimum LSF with a chosen ansatz

Performance of the Ansatz Functions

For qualifying the ansatzes (see table), we computed the LSFs for each paper and each angle. Figure 9 shows the mean RMSD (averaged over all angles) and their standard deviations. For all papers, $RMSD_1$ (Gaussian ansatz) shows the poorest performance. The best results can be found for the ansatzes 3 and 4.

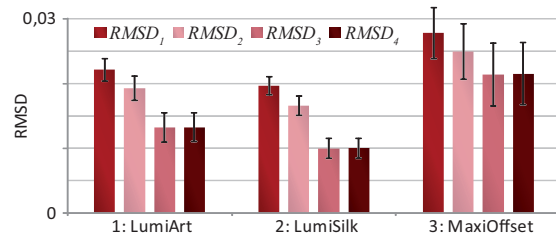


Figure 9. Mean RMS difference for the three sample papers

For the following calculations, the ESFs were averaged over all angles before performing the computations. In figure 10 we juxtapose the reference ESF, the mean sample ESF of paper 2, and the approximated ESFs E_j . Here the ansatzes 3 and 4 clearly perform best.

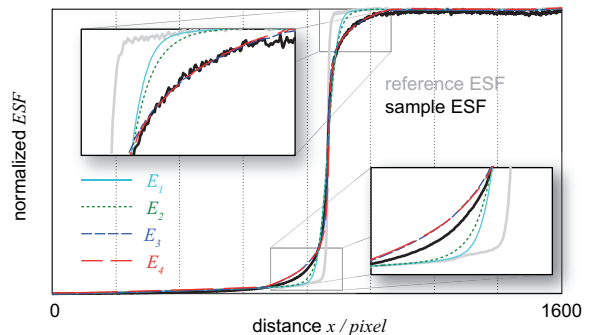


Figure 10. Reference ESF, sample ESF and approximated ESFs

Improvements on Optical Dot Gain

For the following investigations we chose ansatz 3 that performs well for all papers. In order to verify the measurements we compared spectrophotometrically measured colors of printed AM halftones (black ink, 80 L/cm) with predictions calculated with

and without ODG. For this purpose we designed a simplified first principle model with an ODG module that is based on measured PSFs. We do not expect to perfectly predict the color since the model is based on many simplifications, but we want to show that the accuracy improves if ODG is considered.

The measured samples were offset printed halftones of total values $\varphi = 20\%$, 40% , and 60% . Measurements of fulltones and paper white served for calculation of the spectral transmission of the ink $\tau(\lambda)$. For each halftone, the area that is covered with ink was measured with a digital microscope to get the geometrical ink coverage φ . It is a precondition, that ODG does not influence the measured geometrical ink coverage. Although it is not likely that this is valid with the chosen measuring method, it is the best method known for this application. Transmission of the ink and geometrical ink coverage were inputs for simulating the color of the measured patches. All spectral measurements were conducted with $0^\circ/45^\circ$ geometry.

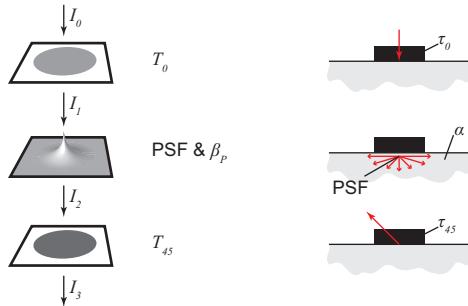


Figure 11. Three steps of color simulation of halftones

Our first principle model is designed according to figure 1 with some simplifications.

Mechanical Dot Gain: For simulating the color of the halftones, we made the simplified assumption that the printed dots are perfectly circular and evenly thick. The diameter of the dots was calculated using geometrical ink coverage and halftone frequency of the measured samples.

Optical Dot Gain: The ODG model is based on the traverse of incident light through the printed substrate (surface effects are not considered in our model). The steps are shown in figure 11: First the light beam hits the ink layer in 0° angle, according to the measuring geometry of the spectrophotometer. If there is a dot, the light is partially absorbed in the ink, otherwise it passes through without any change. This can be described by the transmission matrix T_0 whose elements $t_{0,ij}$ have the value τ_0 for the dots and are 1 otherwise.

Next, the light beam penetrates the paper. It is scattered, described by the PSF, and partially absorbed by the paper, described by its reflectance β_p .

In the last step the light passes the ink layer again. We consider only light that emerges in 45° angle so that it can be detected by the spectrophotometer. This is modeled by the transmission matrix T_{45} that considers the longer way through the ink by a lower transmission factor τ_{45} for the dots. This way, the overall transmission τ has to be divided into a transmission for 0° incidence τ_0 and for 45° emission τ_{45} in a way that considers the different geometric lengths of the two paths.

For a constant illumination I_0 , the three steps can be de-

scribed with equations 7-9, as shown in figure 11 on the left.

$$I_1 = \{e_{1,ij} = i_{0,ij} \cdot t_{0,ij}\} = \begin{bmatrix} i_{0,11} \cdot t_{0,11} & i_{0,21} \cdot t_{0,21} & \dots \\ i_{0,12} \cdot t_{0,12} & i_{0,22} \cdot t_{0,22} & \\ \vdots & & \ddots \end{bmatrix} \quad (7)$$

$$I_2 = \beta_p \cdot (i_1 \otimes PSF) \quad (8)$$

$$I_3 = \{i_{3,ij} = i_{2,ij} \cdot t_{45,ij}\} \quad (9)$$

For calculations without dot gain, equation 8 was reduced to:

$$I_2 = \beta_p \cdot I_1 \quad (10)$$

The table below shows the results of the color calculations as CIELAB values with $D65/2^\circ$ and the deviations from the measured colors as ΔE_{ab}^* . Obviously, the calculation of ODG according to our measurements improves the predicted color. The only exception is the 60% patch of paper 2 (LumiSilk). The reason might be the uncertainty of measurement for the middle halftones. Here, a slight change of diameter of the dot has the biggest effect on the measured area coverage. Probably, the geometrical ink coverage has been overestimated for the 60% patch and this way the additional ODG does not improve the result.

Colorimetric results for measured halftone patches and simulated colors with (+) and without (-) optical dot gain (ODG)

		measured			- ODG	+ ODG
		L^*	a^*	b^*	ΔE_{ab}^*	ΔE_{ab}^*
1: Lumi- Art	20%	78.9	0.2	-2.0	3.2	0.8
	40%	61.1	-0.4	-1.6	3.5	1.1
	60%	40.9	-0.9	-0.9	4.4	1.0
2: Lumi- Silk	20%	83.4	0.1	-1.2	2.3	0.6
	40%	70.0	-0.3	-0.9	3.4	0.6
	60%	54.1	-0.7	-0.6	1.4	2.6
3: Maxi- Offset	20%	82.4	1.1	-3.9	3.0	1.1
	40%	70.3	0.6	-2.6	4.5	1.4
	60%	57.4	0.1	-1.3	1.9	1.7

The results are promising and show the usefulness of our measurements of the light's scattering properties for the investigated papers. Obviously, paper 1 and paper 2 share very similar scattering properties. Paper 3 has higher ODG. The ΔE_{ab}^* show that there are still deviations from the measured CIELAB values. This can be due to the various simplifications of our model and the measuring setup that does not exclude surface effects.

The influence of diffuse and specular surface reflections was quantified in a further investigation. We measured the ESFs of reference materials - a white ceramic tile and opal glass with a matt and a glossy surface for each material. The measurements show that the assumption of insignificant specular surface reflections is not valid. Hence, we believe that the use of orthogonal polarization filters will enhance the results of future investigations.

Conclusions

Light scatter in paper plays an important role in designing first principle printer models. The measurement of light scatter and the resulting optical dot gain is a challenge. Nevertheless, a better understanding of these physical effects enables us to develop more accurate first principle models. We believe that such

models may reduce the number of required test patches for accurately predicting printed colors to an acceptable amount.

In this paper we present an enhanced measurement setup for quantifying light scatter in paper. It is generally applicable to detect local anisotropies of light scatter within paper. The major advantages are:

1. The exact position of the edge of the dark zone is not needed for deriving the PSF.
2. The sample holder allows for simple and accurate focusing. Angular anisotropic scattering can be measured. Isolines of the measured ESF, displayed in a polar diagram, can be used for describing anisotropies.
3. Coated and uncoated papers can be distinguished by different mean radii in the polar diagram.

Due to the small number of measurements, we cannot draw conclusions on the global scatter properties of the examined papers. But it is very likely that the local anisotropies will smooth in a global investigation. Nevertheless, there are still some factors that might bias the measurement of light scatter. Since the measurement setup consists of a $0^\circ/0^\circ$ measurement geometry, specular and diffuse surface reflections can influence the measurement results. First measurements show, that the influence of surface reflections can be reduced to a negligible amount when using two orthogonal polarization filters.

We state that the RMSD between measured ESF and computed ESF is a measure for the accuracy of the approximated LSF. The results show that there is still some room for improvement concerning the ansatz functions for the PSFs and LSFs. Finding the optimal ansatz function shall be investigated in future.

A simple model was presented to calculate halftone colors with and without optical dot gain from the approximated PSF for a given AM dot pattern. We compared predicted with measured colors of printed halftone patches on three sample papers. The accuracy of predictions could be enhanced by incorporating optical dot gain. We expect an improved prediction performance by enhancing the measurement setup and evaluation algorithms. Thus, optical dot gain could be estimated without printing any test patches. The results can be assigned to FM patterns as well. It is very likely that the calculated color differences will differ from those presented here because FM patterns are more sensitive to ODG.

In future investigations, different papers shall be measured with the proposed polarization method. The results are to be verified with printed samples of different AM and FM grids and different printing techniques. Another aspect of the model will be the ink thickness distribution (in contrast to the solid dot model presented here) and its influence on the printed color as well as multi-ink systems.

References

- [1] D.R. Wyble, R.S. Berns, "A critical review of spectral models applied to binary color printing," *Color Res Appl*, 25, 4 (2000).
- [2] F.R. Ruckdeschel, O.G. Hauser, "Yule-Nielsen effect in printing: a physical analysis," *Applied Optics*, 17, 3376 (1978).
- [3] G. Fischer, et al., "Ein physikalisches Modell für die Beschreibung von Lichtstreuungsprozessen," *Die Farbe*, 30, 199 (1982).
- [4] F. Berg, *Isotrope Lichtstreuung in Papier - Neue Überlegungen zur Kubelka-Munk-Theorie* (Technische Hochschule Darmstadt, 1997).
- [5] P. Kubelka, F. Munk, "Ein Beitrag zur Optik der Farbanstriche," *Zeitschrift für technische Physik*, 11a, 593 (1931).
- [6] H.E.J. Neugebauer, "Die theoretischen Grundlagen des Mehrfarbendruckes," *Zeitschrift für wissenschaftliche Photographie*, (1937).
- [7] H.E.J. Neugebauer, "The Theoretical Basis of Multicolor Letterpress Printing," (Translated by D. Wyble and A. Kraushaar), *Color Res Appl*, 30, 322 (2005).
- [8] J.A.S. Viggiano, *The Color of Halftone Tints*, TAGA Proceedings, pg. 77-82. (1985).
- [9] J.A.S. Viggiano, *Modeling the Color of Multi-Colored Halftones*, TAGA Proceedings, pg. 44-62. (1990).
- [10] J.A.C. Yule, W.J. Nielsen, *The Penetration of Light into Paper and its Effect on Halftone Reproduction*, Proc. of the 3rd Annual Technical Meeting, TAGA, pg. 65. (1951).
- [11] R. Rolleston, R. Balasubramanian, *Accuracy of Various Types of Neugebauer Model (IS&T/SID, Scottsdale, Ariz., 1993)* pg. 32-36.
- [12] G.L. Rogers, "Optical Dot Gain in Halftone Print," *Jour. Imaging Sci. and Technol.*, 41, 643 (1997).
- [13] J.S. Arney, et al., "An MTF Analysis of Paper," *Jour. Imaging Sci. and Technol.*, 40, 19 (1996).
- [14] J.S. Arney, et al., "Modeling the Yule Nielsen Halftone Effect," *Jour. Imaging Sci. and Technol.*, 40, 3 (1996).
- [15] J.S. Arney, et al., "Kubelka-Munk Theory and the MTF of Paper," *Jour. Imaging Sci. and Technol.*, 47, 339 (2003).
- [16] C. Ackermann, et al., *Einfluss von Lichtstreuung und Lichtabsorption auf die Bildwiedergabe gedruckter Rasterflächen*, (AiF-No. 12395N) 2002.
- [17] M. Walter, *Methode zur Messung orthotroper Lichtstreuung in grafischen Papieren* (Technische Universität Darmstadt, 2009).
- [18] G.D. Boreman, *Modulation Transfer Function in Optical and Electro-Optical Systems* (SPIE Press, Bellingham, WA, 2001) pg. 69.

Author Biography

Kathrin Happel received her MS in Mechanical Engineering from Technische Universität Darmstadt (Germany) in 2006. Currently, she is research assistant and doctoral candidate at the Institute of Printing Science and Technology at the Technische Universität Darmstadt. Her research focuses on physically based spectral printer models (multi ink) and measuring methods for the acquisition of model parameters.

Marius Walter received his MS in Mechanical Engineering from Technische Universität Darmstadt (Germany) in 2009. In his thesis he developed a method for measuring orthotropic light scattering for graphic arts papers.

Philipp Urban has been head of an Emmy-Noether research group at the Technische Universität Darmstadt (Germany) since 2009. His research focuses on color science and spectral imaging. From 2006-2008 he was a visiting scientist at the RIT Munsell Color Science Laboratory. He holds a MS in mathematics from the University of Hamburg and a PhD from the Hamburg University of Technology (Germany).

Edgar Dörsam has been full Professor and Director of the Institute of Printing Science and Technology at the Technische Universität Darmstadt, Germany since 2003. From 1994-2003 he was responsible for research and development at MAN Roland AG in Offenbach, Germany. He has more than 30 patents and is member of IS&T, VDD, VDI and OE-A. He holds a MS and a doctoral degree in Mechanical Engineering from Technische Universität Darmstadt.